CONTROLLING THE THERMAL ENVIRONMENT OF UNDERGROUND POWER CABLES ADJACENT TO HEATING PIPELINE USING THE PAVEMENT SURFACE RADIATION PROPERTIES

Dardan O. KLIMENTA [a*], Bojan D. PEROVIĆ [a], Jelena Lj. KLIMENTA [b], Milena M. JEVTIĆ [c], Miloš J. MILOVANOVIĆ [a], and Ivan D. KRSTIĆ [a]

[a] Faculty of Technical Sciences, University of Priština in Kosovska Mitrovica, K. Mitrovica, Serbia
[b] Independent consultant in the field of urban and spatial planning, Niš, Serbia
[c] Technical Faculty in Bor, University of Belgrade, Bor, Serbia

This paper shows how the pavement surface radiation properties can be used to control the thermal environment of 110 kV underground cables in order to increase their ampacity. It is assumed that the ampacity is additionally affected by the cable bedding size and an underground heating pipeline. Thanks to an experimental apparatus, some useful data were collected for the validation of two different FEM-based models that predict the effect of the pavement surface radiation properties on the cable ampacity. The first model corresponds to the experimental apparatus and actual indoor conditions, while the second one correspond to the theoretical case and assumed outdoor conditions (taking into account the thermal effects of solar radiation, cable bedding size and heating pipeline). This paper examines two possible cases of outdoor conditions, one corresponding to summer period (the most unfavorable ambient conditions) and another one corresponding to winter period (the most common winter conditions in Serbia). This proposed new method is based on the experimental data and generalized using the FEM in COMSOL. It is found that the ampacity of the considered 110 kV cable line can be increased up to 25.4 % for the most unfavorable ambient conditions and up to 8 % for the most common winter conditions.

Key words: *ampacity, cool pavement, finite element method (FEM), heating pipeline, power cable, surface radiation properties*

Introduction

By controlling the thermal environment, an existing underground cable line may be able to carry more electricity. Three different methods were used to control the thermal environment of underground cable lines. These methods are [1]: the use of special cable beddings (selected or stabilized), the use of forced-cooling cable systems (separate pipe cooling, integral pipe cooling or internal oil cooling), and irrigation of cable beddings.

Cool pavements (also known as solar reflective cool or high albedo pavements) can reduce the absorption of heat from solar radiation and stay cooler in the sun than traditional dark pavements (also known as hot or low albedo pavements), such as conventional black asphalt and asphalt concrete. Pavement reflectance can be enhanced by means of reflective aggregates, binders or surface coatings, as well as clear binders. Cement-based grouting materials utilizing recycled ceramic waste powder were found to reduce the surface temperature of asphalt-pavement by 10-20 °C when the asphalt-pavement reached daytime temperatures of 60 °C or more [2]. In addition to this, a cool pavement seal was found to reduce the surface temperature of asphalt-pavement by 11.1-13.9 °C when the asphalt-pavement reached 71.1 °C in summer [3]. Cooler pavement surfaces are especially

[*] Corresponding author, e-mail: dardan.klimenta@pr.ac.rs

important because they transmit less heat to the surrounding air, reducing the urban heat island effect (UHI effect). This technological innovation can be applied not only to the UHI effect, but also to controlling the thermal environment of underground power cables in order to increase their ampacity. This paper introduces the use of cool pavements as a new method for controlling the thermal environment of underground cables, which also represents the main purpose of the study.

With the exception of [4], the existing literature currently does not identify cool pavements as means to control the thermal environment of underground power cables. The effect of the earth surface on an underground cable line usually comes down to the natural convection [5] or to a combination of the natural convection and radiation by accounting for the influence of heat from solar radiation [6]. How thermal conductivity of cable bedding materials affects the behaviour of underground power cables was reported in [7,8], while data on the thermal effect of heating pipeline can be found in research articles like [9]. However, there is a possibility to change temperatures of cables and their surroundings by the pavement surface radiation properties.

This paper is based on the experimental results obtained with an apparatus and the assumption that it is planned to install one 110 kV underground cable line parallel to the concrete duct of an underground heating pipeline whose external dimensions are 1.9 m and 1.185 m [9]. It is assumed that the trench along the entire length of the cable line is completely filled with quartz sand and paved with a layer of solid material whose surface absorbs less heat from the sun than it emits to the ambient. Quartz sand would provide good conduction of heat from the cables to the cool pavement surface, while the paved surface of the trench would establish approximately unchangeable convection and radiation boundary conditions along the entire cable route. Moreover, it is assumed that single-core 110 kV cables are installed in trefoil formation where the axial spacing between the individual cables equals one cable diameter, that the heating pipeline is constructed in accordance with the relevant standards, that the outer surface temperature of the heating-pipe duct is constant and equal to 50 °C, and that the soil temperature at a reference distance is 20 °C in summer and 10 °C in winter.

The simultaneous impact of the cool pavement, cable bedding size and heating pipeline on the 110 kV distribution cable line is then analyzed. This paper also describes the conditions under which the cool pavement surface may be used as a mean to control the thermal environment around the cables, as well as their ampacity. Also, in order to ensure the mesh independence, a mesh sensitivity analysis was conducted for FEM-based simulations. Furthermore, there was no optimization of the cable bedding size, but it is assumed that the width of the soil zone intended for laying cables equals 1.2 m [4]. According to the DIN VDE standards, the ABB AXLJ 1×1000/190 mm^2 110 kV cable considered herein corresponds to the NA2XS(FL)2Y type.

Experimental setup

Fig. 1 illustrates the schematic diagram of experimental setup for investigating the pavement surface radiation properties. The main purpose of this apparatus is to simulate the effect of the pavement surface emissivity on the thermal environment of underground power cables in the absence of solar radiation and heating pipeline. The authors considered the following experimental cases: (a) pavement made of concrete blocks covered by some river sand acting as dust, (b) concrete pavement coated with acrylic white paint, and (c) concrete pavement coated with acrylic black paint. The concrete blocks had a height of 0.065 m, a width of 0.1 m and a length of 0.2 m. The radiation properties of concrete surface and acrylic paints are listed in tab. 1. Along with these surfaces, tab. 1 also contains some of the materials and paints which can be used as cool pavements for controlling the thermal environment of underground power cables. The surfaces of the selected materials and paints absorb less heat from the sun than they emit to the ambient, i.e. each of these surfaces has the solar absorptivity α lower than its emissivity ε.

The experimental apparatus was composed of a container made from a used refrigerator, whose walls consisted of 2-mm-thick polystyrene inside, 1-mm-thick metal sheet on the outside, with 47- or 57-mm-thick polyurethane foam between as a thermal insulation. Only one side of the container was constructed of 50-mm-thick polyurethane foam slab sandwiched between two 30-mm-thick slabs of styrodur. It was open on top and was filled with river sand up to 0.075 m below the top edges of the container to simulate the case when the cable trench is completely filled with bedding material. Outer

dimensions, i.e. length, width and height of this container were 1.17, 0.6 and 0.5 m, respectively. For all the outer surfaces of the container, it was found that the heat transfer coefficient amounts approximately 3 W/m^{2}K. Thermal conductivities of materials used for experiments and simulations are given later in this paper.

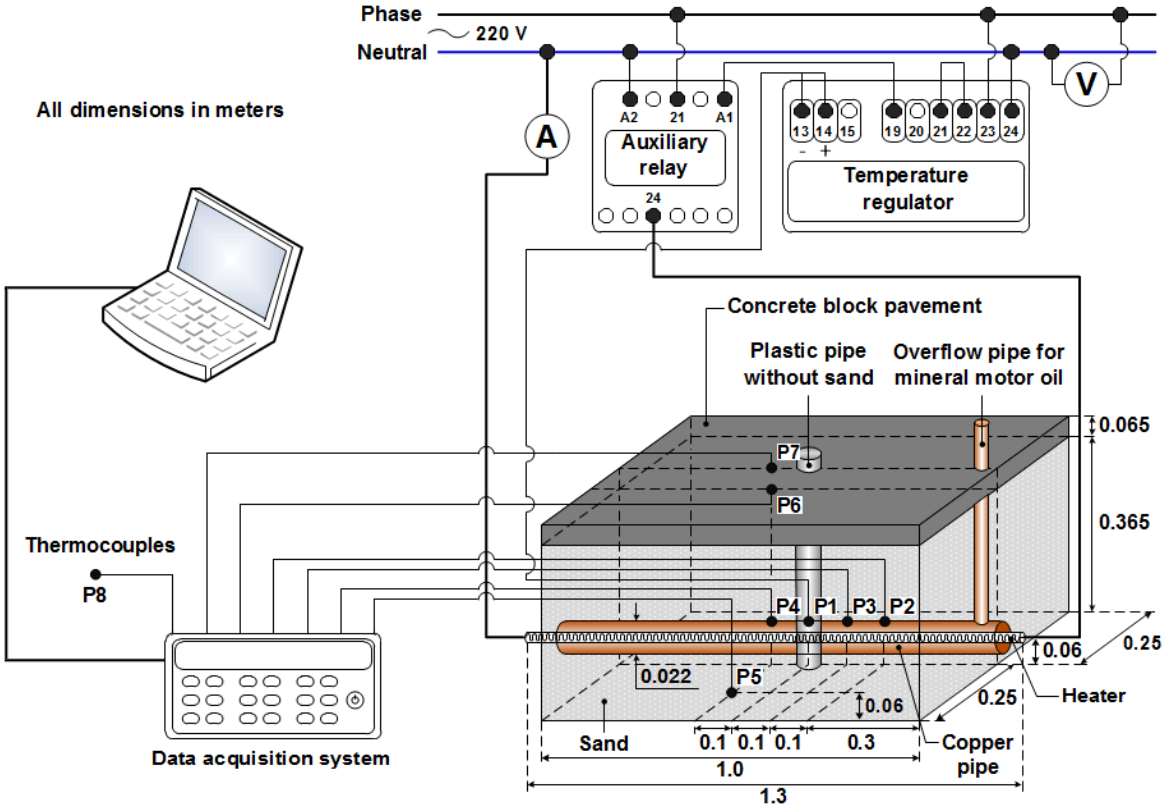

Figure 1. Schematic diagram of experimental setup

Table 1. Radiation properties of pavement surfaces and paints

Material or paint	α [–]	ε [–]	Material or paint	α [–]	ε [–]
Concrete block	0.56-0.69	0.94	Limestone, light	0.33	0.9-0.93
Acrylic white paint	0.26	0.9	Marble, white	0.44	0.9-0.93
Acrylic black paint	0.97	0.91	Limestone, dark	0.53	0.9-0.93
Magnesium oxide white paint	0.09	0.9	Clay tiles, red or brown	0.60-0.69	0.85-0.95
Brick, light	0.25-0.36	0.85-0.95	Asphalt	0.87	0.93

Heat sources located in a single ABB AXLJ 1×1000/190 mm^2 110 kV cable during operation were modeled by a horizontal copper pipe of a smaller outer diameter, which was also equipped with a tubular heater and an overflow pipe. The overflow pipe is used to set the level of mineral motor oil in the horizontal copper pipe. The heater had a total nominal power of 0.8 kW and a length of 1.3 m. It was mounted in the center of the copper pipe and connected to the low-voltage power supply network. The connection was realized by means of a microprocessor-based temperature regulator (NIGOS 1011P) and an auxiliary relay (SCHRACK multimode relay MT 326230), as shown in fig. 1.

In these experiments, the J-type thermocouples were installed on the copper pipe in four different locations (P1 in the air, and P2, P3 and P4 in the sand), including the inner lateral surface of the container (P5), the lower surface of the pavement (P6), the upper surface of the pavement (P7), and the surrounding air (P8). The thermocouple P1 was directly connected to the measuring input of temperature regulator. The temperatures measured by the thermocouples P2-P8 were collected through a data acquisition system (Agilent 34970A) and connected to a laptop to collect the data. Temperatures

of the outer lateral surfaces of the container were measured by an infrared thermometer (with an accuracy of ±2.0 °C below 100 °C and ±2.0 % above 100 °C). There was also one Pt100 temperature sensor to monitor the internal temperature in the module of the data acquisition system, which is used as a reference/cold junction temperature. During the runs without river sand, the FLIR i3 thermal imaging camera was used for inspection of the heater and for selection of the positions for the thermocouples P1-P4.

In order to study the steady-state temperature distribution for different pavement surfaces without the effects of the sun and heating pipeline, temperatures at 8 hours from the start of each experiment were noted. One experiment ended once a period of 8 hours has elapsed. The thermal effects of the sun, cable bedding and heating pipeline are subsequently defined and added through COMSOL simulations of the problem.

Procedure and experimental results

The temperature at points P2-P4 was controlled by adjusting the temperature at point P1 with an error less than 1 °C for ambient temperatures 0-50 °C. A specified control temperature on the outer surface of the copper pipe part enclosed by the vertical plastic pipe was fixed at 66 °C. When the container was without river sand, the points at which the temperatures were lower than 66 °C were selected for the thermocouples P2-P4. Then, after the addition of sand, the temperatures at points P2-P4 were increased by a few degrees Celsius adjusting the thermal environment as closely as possible in accordance with the temperature at point P1. This is expected because the heat transfer on the outer surface of the copper pipe was replaced by conduction alone. Along with application for the controlling, the thermocouple P1 was also used for measurement. The temperature of the surrounding air was adjusted at 23 °C with an accuracy of ±1.5 °C.

The temperatures at points P1-P8 and the average temperature of the outer lateral surfaces of the container obtained for the three cases (a-c) are listed in tab. 2. Tab. 2 also contains the specified control temperature and average temperature of the outer surface of the copper pipe (obtained by averaging the measured values at points P2-P3).

Table 2. Experimental results

Specified control temperature	Measured temperature in degrees Celsius									
	Thermocouple or outer surface of …									
is 66 °C	**P1**	**P2**	**P3**	**P4**	**Copper pipe ***	**P5**	**Container ***	**P6**	**P7**	**P8**
Case (a)	65.0	62.9	64.4	68.4	65.2	31.4	22.6	24.8	23.8	21.8
Case (b)	65.0	63.5	65.1	69.2	65.9	32.3	24.6	26.9	26.2	24.2
Case (c)	65.0	63.4	64.9	69.0	65.8	33.3	24.4	27.3	26.3	23.8

* Average values

Numerical modeling

This paper considers two cases of steady-state thermal analysis, using the laboratory and outdoor conditions. The steady-state thermal FEM models and associated analysis are based on the following equation [4,10]:

$$\frac{\partial}{\partial x}\left(k\frac{\partial T}{\partial x}\right)+\frac{\partial}{\partial y}\left(k\frac{\partial T}{\partial y}\right)+Q_v=0 \tag{1}$$

where k is the thermal conductivity in W/mK, T – the unknown temperature in K, x, y – Cartesian spatial coordinates in m, and Q_v – the volume power of heat sources in W/m^3. In addition, thermal FEM analysis will be non-linear due to the radiation boundary condition.

Computational domains which will be used for confirmation of the initial assumption that the ampacity of underground power cables can be controlled by the pavement surface radiation properties are given in figs. 2(a) and 2(b). Fig. 2(a) shows the domain corresponding to the

experimental setup, while fig. 2(b) shows the domain for the case when the cables are laid in the bedding of a standard size 1.2 m × 0.65 m. Compared with the computational domain in fig. 2(a), the domain shown in fig. 2(b) is large and selected in accordance with the rule saying that external boundaries of a computational domain should be positioned in places where the constant temperature and homogenous boundary conditions are satisfied simultaneously [10]. Moreover, the dimensions of the domain in fig. 2(b) are about four times larger than those recommended in IEC TR 62095 [11].

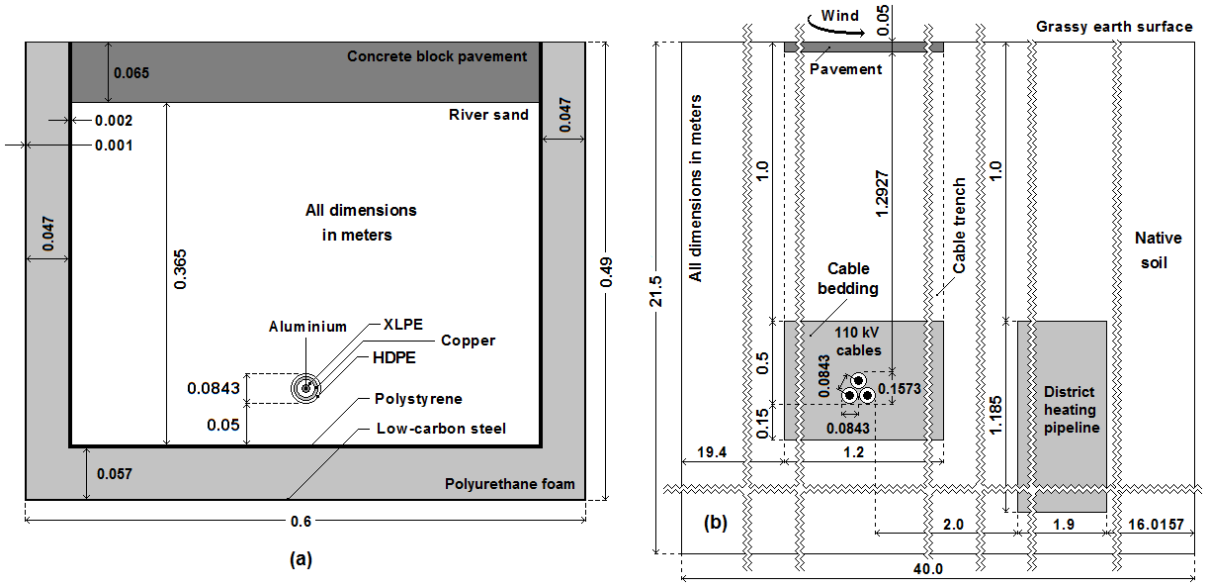

Figure 2. Presentation of computational domains: (a) domain corresponding to the experimental setup; and (b) domain for the case of cable bedding size 1.2 m × 0.65 m

For the purposes of thermal FEM analysis using COMSOL, the ABB AXLJ 1×1000/190 mm^2 110 kV cable is modeled by an equivalent construction composed of the aluminium conductor, cross-linked polyethylene (XLPE) insulation, copper screen and outer polyethylene (PE) sheath with outer diameters 0.0384, 0.0713, 0.0767 and 0.0843 m [10], respectively. According to [10], the equivalent construction represents the following: the semi-conducting screens and swelling tapes under the metal screen are modeled by XLPE; the swelling tapes over the metal screen and water-sealing aluminium layer are modeled by an equivalent metal screen with thermal properties of copper; and the conducting high-density polyethylene (HDPE) layer is added to the block representing the outer protective sheath.

The commercial software COMSOL Multiphysics v 4.3 [12] was used to solve a second-order nonlinear system of partial differential equations of the form (1). The meshes generated automatically in COMSOL for the computational domains in figs. 2(a) and 2(b) were composed of 28671 and 5969 linear triangular elements, respectively. These linear triangles were connected in 14931 and 3034 common nodes and approximated the shape of domains in figs. 2(a) and 2(b), respectively. The meshes were finer for thin layers (inner liners, metal sheet, XLPE insulations, copper screens and outer PE sheaths) compared to other ones. The remaining rules of mesh generation are described in [12].

In order to ensure the mesh independence, i.e. an acceptable degree of mesh sensitivity [7], the authors tracked the temperature in the center of each aluminium conductor and the load current. The number of triangular elements was varied from 28671 to 458736 and from 5969 to 95504 for the domains in figs. 2(a) and 2(b), respectively; and the temperature differences were lower than 0.005 °C. To ensure that the steady-state thermal analysis depends to a very small extent on the number of elements or nodes, the temperatures at the axes of the conductors were tracked. The variation in temperature was lower than 0.005 °C when the number of nodes was varied from 14931 to 231747 for the domain in fig. 2(a) and from 3034 to 47950 for the domain in fig. 2(b). Accordingly, the variation in temperature could not affect the corresponding load current. Hence, meshes with 14931 and 3034 nodes were used for the domains in figs. 2(a) and 2(b), respectively.

FEM simulations of temperature field distributions over the domain in fig. 2(a) are conducted for pavement made of concrete blocks covered by some river sand acting as dust, as well as concrete pavements coated with acrylic white and black paints. Simulations over the domain shown in fig. 2(b) are conducted for the following five pavements: asphalt coated with magnesium oxide white paint, light bricks, light limestone, concrete blocks and uncoated asphalt. The pavement materials are selected so that their solar absorptivities and emissivities are assumed to be equal to the lower bounds of the corresponding ranges of possible values from tab. 1.

The thermal conductivities k of all the materials and the electrical conductivity of aluminium are necessary for the steady-state thermal FEM analysis. All the necessary material properties required by this analysis are constant and selected so that the obtained results are optimistic from the engineering point of view. Hence, the values of the thermal and electrical properties which correspond respectively to the associated dried-out states (of the native soil and the cable bedding) and the continuously permissible temperature T_{cp} are taken into consideration. Continuously permissible temperature of the considered XLPE cable is T_{cp}=90 °C. The values for k are taken from related literature and represented in tab. 3.

Table 3. Thermal conductivity of all used materials

Material	k [W·m^{-1}·K^{-1}]	Material	k [W·m^{-1}·K^{-1}]
Polystyrene	0.13	Limestone, light, 2180 kg/m^3	1.5
Low-carbon steel	43	Concrete block, 2000 kg/m^3	1.3
Polyurethane foam	0.025	Cable bedding	1
Styrodur	0.033	Native soil	0.4
River sand, with particles smaller than 3 mm, 1365 kg/m^3	0.4	Aluminium	239
Asphalt, 2300 kg/m^3	1.2	Copper	385
Brick, light, solid, 2600 kg/m^3	1	PE, HDPE and XLPE	0.286

The volume power of heat sources located in the conductor Q_v with a diameter of d_1=0.0384 m and with a geometric cross-section area of S'_c =1158.117·10^{-6} m^2 is

$$Q_v = \frac{R_{ac}(T_{cp})}{S'_c} \cdot I^2 \tag{2}$$

where $R_{ac}(T_{cp})$ =40.91094·10^{-6} Ω/m is the a.c. resistance per unit length of the conductor at temperature T_{cp}, and I – the load current in A. The a.c. resistance of the 110 kV cables is calculated taking into account the skin and proximity effects [10]. Volume powers of heat sources located in the cable insulations are equal to zero due to the fact that, in accordance with the IEC 60287 standard, the associated dielectric losses (per unit length in each phase cable) are equal to 0.362647 W/m, which is negligible for 110 kV cables [10,13]. Volume powers of heat sources located in the metal screens of the 110 kV cables are also equal to zero because of the cross-bonding of metal screens.

It is common to determine the cable ampacity for the most unfavorable ambient conditions in summer such as: (i) temperature of the air contacting the earth surface $T_a = 40$ °C; (ii) wind velocity, i.e. velocity of the air near the earth surface of $v_a = 0.22$ m/s; (iii) solar irradiance incident on the earth surface $Q_{S,s} = 1000$ W/m^2; (iv) temperature of referent soil of 20 °C; and (v) thermal conductivities of the cable bedding and native soil whose values correspond to their dried-out state, i.e. 1 W/mK and 0.4 W/mK, respectively. These conditions are very similar to those used in [10]. However, it is quite common for colder days to apply the following ambient conditions: $T_a = 5$ °C, $v_a = 0.22$ m/s, $Q_{S,s} = 1000$ W/m^2, temperature of referent soil of 10 °C and thermal conductivities of the cable bedding and native soil in the dried-out condition (that is, 1 W/mK and 0.4 W/mK). The 110 kV cables will be analyzed under these boundary conditions, as well as under the experimentally determined ones.

The zero heat flux (homogenous or adiabatic) boundary condition is used to model boundaries surrounding the left-hand, right-hand and bottom sides of the computational domain in fig. 2(b) (with regard to the earth surface):

$$k \cdot \frac{\partial T}{\partial n} = 0 \tag{3}$$

where a constant temperature boundary condition $T = T_0(x, y) = 293.15$ K (for the summer period) or $T = T_0(x, y) = 283.15$ K (for the winter period) should also be satisfied simultaneously [10]. In addition, T and T_0 are the unknown and specified temperatures of the corresponding surfaces (model boundaries) in K, respectively.

The four edges representing the exterior of the heating-pipe duct in fig. 2(b) are also modeled by the constant temperature boundary condition, i.e. by the temperature:

$$T = T_0(x, y) = 323.15 \text{ K} \tag{4}$$

In this way, the thermal effect of heating-pipe duct on underground cables is generally not modeled accurately enough for the summer period. Namely, the boundary condition (4) corresponds to the winter period. Therefore, by acting in such way, the obtained ampacities will be safe from the engineering point of view.

In numerical models under consideration, the heat transfer along the earth and pavement surfaces is represented by a combination of the following boundary conditions:

- The convection boundary condition [4,10]:

$$k \cdot \frac{\partial T}{\partial n} = h \cdot (T - T_a) \tag{5}$$

- The radiation boundary condition [4,10,14]:
  (i) for the laboratory/indoor conditions

$$k \cdot \frac{\partial T}{\partial n} = \varepsilon \cdot \sigma_{SB} \cdot (T^4 - T_a^4) \tag{6}$$

  and (ii) for the outdoor conditions

$$k \cdot \frac{\partial T}{\partial n} = \varepsilon \cdot \sigma_{SB} \cdot T^4 - \alpha \cdot Q_{S,s} \tag{7}$$

  where T is the unknown temperature of the pavement or earth surface in K, $\alpha = 0.6$ and $\varepsilon = 0.94$ for a dry grassy surface [15-18], $h = 12.654$ W/m^{2}K for a dry grassy surface when $v_a = 0.22$ m/s [17,18], $h = 8$ W/m^{2}K for a pavement surface when $v_a = 0.22$ m/s [10,17] and $\sigma_{SB} = 5.67 \cdot 10^{-8}$ W/m^{2}K^4 is the Stefan-Boltzmann constant. The coefficient h, which appears in the equation (5), takes into account heat transfer due to convection between the pavement or earth surface and the ambient air. For the laboratory/indoor conditions, the wind velocity was of 0 m/s. Other values for the coefficients α and ε are given in tab. 1.

It is assumed in this paper that the convection coefficient for a grassy surface has a greater value than the one for a pavement surface. This is caused by some loss of heat due to evaporation of water from the grassy surfaces, which does not exist along the pavement surfaces [17,19]. Therefore, the effect of evaporation on the heat transfer due to convection between the earth surface and the ambient air is introduced by the corresponding coefficient, whose value is estimated using the empirical correlation $h = 11.4 + 5.7 \cdot v_a$ from [18] for a wind velocity of 0.22 m/s relating to a clear sunny and quiet day where wind condition is low and fairly constant [17]. In addition, using the empirical correlation $h = 7.382 + 1.925 \cdot v_a^{0.75}$ from [10], it is found that the wind velocity of 0.22 m/s corresponds to the average convective heat transfer coefficient of 8 W/m^{2}K [17].

Experimental validation of numerical modeling

Some of the results obtained by simulating the temperature field distribution over the two-dimensional domain in fig. 2(a) are reported in tabs. 4 and 5. Tab. 4 outlines the main results obtained for the actual indoor conditions, while tab. 5 presents the corresponding results obtained for the modified indoor conditions. The terms 'actual indoor conditions' and 'modified indoor conditions' are understood to exclude and include the effect of the sun, respectively. For the domain shown in fig. 2(a), a sequence of simulations is performed with gray, white and black pavement surfaces. The appearance order of the colors in tabs. 4 and 5 follows the sequence of experiments. The surface radiation properties and thermal conductivities appearing in this FEM model are given in tabs. 1 and 3, respectively.

Table 4. Simulation results obtained for the actual indoor conditions, i.e. for T_a=23 °C, v_a=0 m/s, h=7.382 W/m^{2}K and $Q_{S,s}$=0 W/m^2

Pavement surface		Temperature [°C]							Q_v	I
Color	ε [–]	Cable conductor	Cable outer surface		Pavement				[W·m^{-3}]	[A]
					Lower surface		Upper surface			
			Sim *	Diff *	Sim *	Diff *	Sim *	Diff *		
Gray	0.94	77.77	65.00	-0.2	28.21	+3.41	26.13	+2.33	26710	869.55
White	0.90	77.79	65.00	-0.9	28.27	+1.37	26.18	-0.02	26700	869.38
Black	0.91	77.79	65.00	-0.8	28.25	+0.95	26.16	-0.14	26705	869.47
Gray	0.94	90.00	74.33	–	29.37	–	26.83	–	32670	961.68
White	0.90	90.00	74.33	–	29.43	–	26.88	–	32650	961.39
Black	0.91	90.00	74.34	–	29.42	–	26.86	–	32660	961.53

* "Sim" stands for the simulated value and "Diff" for the difference between the simulated and experimental values

Table 5. Simulation results obtained for the modified indoor conditions, i.e. for T_a=23 °C, v_a=0 m/s, h=7.382 W/m^{2}K and $Q_{S,s}$=1000 W/m^2

Pavement surface		Temperature [°C]				Q_v	I
Color	α/ε [–]	Cable conductor	Cable outer surface	Pavement		[W·m^{-3}]	[A]
				Lower surface	Upper surface		
Gray	0.596	69.84	65.00	61.61	61.99	10850	554.21
White	0.289	73.91	65.00	44.65	43.78	18930	732.03
Black	1.070	64.50	65.00	83.98	85.99	210	77.10
Gray	0.596	90.00	80.41	63.38	62.97	20730	766.05
White	0.289	90.00	77.33	46.14	44.65	26790	870.85
Black	1.070	90.00	84.49	86.13	87.14	12740	600.54

When the simulation results from the first three rows of tab. 4 are compared with the corresponding experimental data in tab. 2, the following observations can be made: (i) For each of both temperatures of the cable conductor, in the absence of solar radiation, approximately the same load current is obtained regardless of the color of the pavement surface. (ii) The simulated temperature of the outer surface of the cable is lower by 0.2-0.9 °C than the corresponding average temperature of the outer surface of the copper pipe. (iii) The difference between the simulated temperature of the lower surface of the pavement and its corresponding measured value at point P6 ranges from +0.95 °C to +3.41 °C. (iv) The difference between the simulated temperature of the upper surface of the pavement and its corresponding measured value at point P7 ranges from -0.14 °C to +2.33 °C. The first observation is based on approximately equal values for the emissivity of the three colors, while the remaining three observations indicate a satisfactory level of accuracy on account of the created model. These observations also suggest that the inclusion of solar radiation will give results which adequately quantify the effect of the pavement surface absorptivity on the load current.

As mentioned above, tab. 5 quantifies the effect of the pavement surface absorptivity on the load current. This effect is most pronounced in the case when the pavement is coated with the

acrylic black paint and the temperature of the outer surface of the cable is 65 °C, and minimally pronounced in the case when the pavement is coated with the acrylic white paint and the temperature of the cable conductor is 90 °C. In particular, with the inclusion of solar radiation, the cable ampacity of approximately 961.5 A is reduced by 20.3 % in the case of the gray pavement surface, 9.4 % in the case of the white pavement surface, and 37.5 % in the case of the black pavement surface. Thus, it appears that the radiation properties of a pavement surface above underground power cables can be used to control the ampacity.

Results and discussion

In order to generalize the previous results, the large-size FEM model with 110 kV cables was created and presented in fig. 2(b). The temperature field distributions over this computational domain are calculated for: I – the case of bedding size 1.2 m × 0.65 m without heating pipeline, II – the case of bedding size 1.2 m × 0.65 m with heating pipeline, III – the case of bedding size 1.2 m × 1.6 m without heating pipeline, and IV – the case of bedding size 1.2 m × 1.6 m with heating pipeline. For each of these four cases, a sequence of simulations is performed with the following five materials: asphalt coated with magnesium oxide white paint, light bricks, light limestone, concrete blocks and uncoated asphalt. The surface radiation properties and thermal conductivities of these materials were previously listed in tabs. 1 and 3, respectively.

For the four cases relating to the large-size domain, values for Q_v and I are selected in such a way so that they correspond to asphalt surface radiation properties from tab. 1, thermal conductivity of the asphalt k=1.2 W/mK and continuously permissible temperature of the cables T_{cp}=90 °C, as follows: Q_v=10260 W/m^3 and I=538.93 A – for the case I; Q_v=10510 W/m^3 and I=545.45 A – for the case II; Q_v=11270 W/m^3 and I=564.83 A – for the case III; and Q_v=11480 W/m^3 and I=570.07 A – for the case IV. The remaining input parameters are constant and specified in the preceding sections. The temperatures of the pavement, bedding and cables' conductors which are obtained by simulations of the temperature field distribution over the domain shown in fig. 2(b) for these four cases are given in tab. 6.

Table 6. Effect of pavement surface radiation properties on temperatures of pavement, bedding and conductors for the cases I-IV relating to the large-size domain in fig. 2(b)

Pavement material	Surface radiation property α/ε [–]	Pavement surface [°C]	Bedding close to cables [°C]	Cables' conductors [°C]	Pavement surface [°C]	Bedding close to cables [°C]	Cables' conductors [°C]
		Case I			Case II		
Asphalt + paint	0.100	12.02	70.85	75.73	12.05	72.12	77.03
Brick, light	0.294	25.49	74.81	79.49	25.50	75.36	80.44
Limestone, light	0.367	29.60	75.67	80.51	29.61	76.30	81.38
Concrete block	0.596	43.84	79.69	84.49	43.84	79.96	84.99
Asphalt	0.935	63.78	85.35	90.03	63.76	85.13	90.03
		Case III			Case IV		
Asphalt + paint	0.100	13.36	61.99	67.48	13.43	63.29	69.05
Brick, light	0.294	26.45	67.95	73.44	26.49	69.20	74.58
Limestone, light	0.367	30.44	69.37	74.97	30.48	70.53	76.00
Concrete block	0.596	44.29	75.85	81.25	44.31	76.35	81.84
Asphalt	0.935	63.80	84.71	90.02	63.78	84.61	90.01

Based on the results presented in tab. 6, it can be seen that the temperatures of the pavement, bedding and cables' conductors decrease with decreasing the ratio of absorptivity to emissivity α/ε for the pavement surface. The same applies to all four cases related to the large-size domain in fig. 2(b). Hence, it is possible to increase the cable ampacity by selecting a material or paint

with a lower value of the ratio α/ε. The effect of the ratio α/ε on the cable ampacity will be quantified and presented later in this section. Based on these results, it can also be seen that the effect of the heating pipeline increases with decreasing the ratio α/ε and decreases with increasing the height of the cable bedding. For both cable beddings and the most unfavorable ambient conditions, the thermal effect of the heating pipeline on the pavement, bedding and conductors is negligible and goes up to 1.57 °C. The main reason for such a small effect of the heating pipeline is that the thermal FEM analysis is performed with the minimum separation distance of 2 m between the 110 kV cables and the heating pipeline.

It is clear from tab. 6 that the temperatures of the pavement, bedding and conductors would be decreased significantly by the cable bedding whose dimensions are 1.2 m × 1.6 m. However, the temperature of the soil around the cables was not increased significantly by the heating pipeline. Their effects can best be illustrated using the sizes of the dried, dried-out and extremely-dried-out zones enclosed by the isotherms of 50, 60 and 70 °C [9,10,20], respectively. It should also be observed that the temperature of the 50 °C isotherm is equal to the temperature of the outer surface of the heating-pipe duct. Therefore, it is interesting to compare the results obtained for all four cases related to the large-size domain and for the case when the trench is paved with a cheap and easily available material such as light brick. The 50, 60 and 70 °C isotherms which are obtained by simulations of the steady-state temperature field distribution over the large-size domain for the cases I-IV are presented in fig. 3.

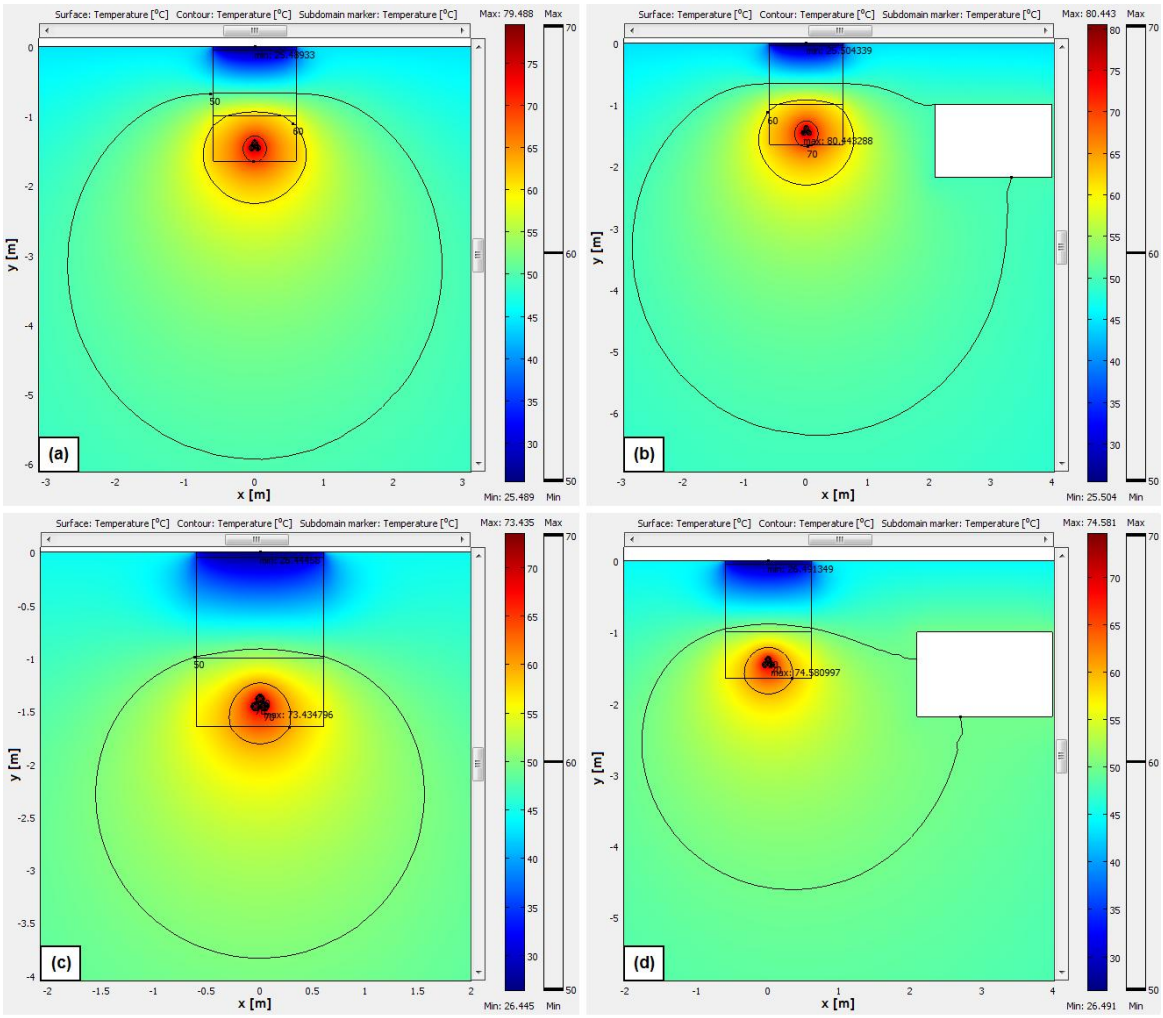

Figure 3. Isotherms of 50, 60 and 70 °C surrounding the dried, dried-out and extremely-dried-out zones around the 110 kV cables which are laid in accordance with fig. 2(b) for: (a) case I; (b) case II; (c) case III; and (d) case IV, where all dimensions are in meters

Based on the sizes of the dried, dry-out and extremely-dried-out zones shown in fig. 3, it is clear that the thermal effect of the heating pipeline is higher when the cable bedding has a smaller size. According to tab. 6, the effect of the heating pipeline on the bedding in close proximity to the cables, expressed in the form of a temperature difference, amounts to 1.27 °C – for the bedding having dimensions 1.2 m × 0.65 m and 1.3 °C – for the bedding having dimensions 1.2 m × 1.6 m. This is contrary to the conclusion which is drawn from the results shown in fig. 3. Therefore, the thermal effect of the heating pipeline on the power cables can be expressed in a more convenient way by the sizes of the dried, dry-out and extremely-dried-out zones.

For the purposes of determining the ampacity of the 110 kV cable line I_{cp}, a sequence of simulations over the large-size domain in fig. 2(b) for the cases I-IV is performed with the most unfavorable ambient conditions and the most common winter conditions, as well as with the radiation and thermal properties (α, ε and k) of the previously selected pavement materials (tab. 6). The values for Q_v are gradually increased from an arbitrary prescribed initial value (for instance 10 kW/m^3) to its continuously permissible value (corresponding to the temperature T_{cp}=90 °C). For the most unfavorable ambient conditions, the volume powers of heat sources Q_v obtained in this way are given in tab. 7. Then, these volume powers of heat sources and eq. (2) are used to calculate the cable ampacities. These ampacities are also given in tab. 7.

Table 7. Volume powers of heat sources located in cables' conductors and cables' ampacities calculated for different thermal environments in summer

Pavement material	Surface radiation property	Volume power of heat sources Q_v and cable ampacity I_{cp}							
		Case I		Case II		Case III		Case IV	
	α/ε	Q_v	I_{cp}	Q_v	I_{cp}	Q_v	I_{cp}	Q_v	I_{cp}
	[–]	[W·m^{-3}]	[A]	[W·m^{-3}]	[A]	[W·m^{-3}]	[A]	[W·m^{-3}]	[A]
Asphalt + paint	0.100	13890	627.06	13980	629.09	18065	715.11	18030	714.42
Brick, light	0.294	12940	605.23	13070	608.27	16265	678.55	16300	679.28
Limestone, light	0.367	12680	599.12	12820	602.42	15815	669.10	15870	670.26
Concrete block	0.596	11670	574.77	11850	579.18	13920	627.73	14040	630.43
Asphalt *	0.596	10260	538.93	10510	545.45	11270	564.83	11480	570.07
Asphalt **	0.935	10810	553.18	10890	555.23	11770	577.22	11830	578.69

* Results obtained for the homogenous boundary condition (3) on the outer sides of the domain

** Results obtained for the constant temperature boundary condition $T=T_0(x,y)$=293.15 K on the outer sides of the domain

Based on the quantification of the effects of the pavement surface radiation properties, cable bedding and heating pipeline on the ampacity of the considered 110 kV cable line, the following can be observed: (i) In comparison with the uncoated asphalt-pavement, the other materials can increase the ampacity of the considered 110 kV cable line up to 88.13 A. (ii) The cable bedding having dimensions 1.2 m × 1.6 m can additionally increase the cable ampacity up to 62.15 A. (iii) The heating pipeline can increase the cable ampacity up to 6.52 A, which is by no means uncommon, but computationally and practically possible. According to the observations (i) and (ii), the ampacity can be increased by 150.28 A if the asphalt-pavement is coated with magnesium oxide white paint and if the cable trench is completely filled with the bedding material. In addition to this, the observation (iii) represents an uncommon result that can be explained in the following way: When the temperature of the outer surface of the heating-pipe duct is constant and equal to 50 °C, the heating pipeline represents a cooler for the cables' conductors having temperatures of approximately 90 °C.

Moreover, the two last rows of tab. 7 contain the results obtained for the homogenous and constant temperature boundary conditions on the left-hand, right-hand and bottom sides of the large-size FEM model. Based on these results, it is obvious that the homogenous boundary condition gives a more accurate solution for the large-size domain and it is also safer from the engineering point of view.

Results obtained for the most common winter conditions in Serbia are presented in tab. 8. These results are generated in the same way as the ones given in tab. 7. Based on tab. 8, it is clear how a heating pipeline affects underground power cables. In particular, these results confirm the fact that

the cable ampacity decreases due to the thermal effect of the heating pipeline. This is contrary to the observation (iii) relating to the results in tab. 7. Therefore, during colder periods, the heating pipeline decreases the cable ampacity by about 36 A, which was expected to occur. In addition, the thermal effects of the radiation properties and bedding size on the cable ampacity are similar to those for the most unfavorable ambient conditions.

Table 8. Volume powers of heat sources located in cables' conductors and cables' ampacities calculated for different thermal environments in winter

Pavement material	Surface radiation property	Volume power of heat sources Q_v and cable ampacity I_{cp}							
		Case I		Case II		Case III		Case IV	
	α/ε	Q_v	I_{cp}	Q_v	I_{cp}	Q_v	I_{cp}	Q_v	I_{cp}
	[–]	[W·m^{-3}]	[A]	[W·m^{-3}]	[A]	[W·m^{-3}]	[A]	[W·m^{-3}]	[A]
Asphalt + paint	0.100	23290	811.97	20990	770.84	28540	898.84	26310	863.01
Brick, light	0.294	22730	802.15	20460	761.04	27490	882.15	25290	846.12
Limestone, light	0.367	22610	800.03	20350	758.99	27320	879.42	25130	843.44
Concrete block	0.596	22040	789.88	19800	748.67	26240	861.86	24090	825.80
Asphalt *	0.935	21190	774.50	18990	733.19	24650	835.34	22570	799.32
Asphalt **	0.935	21190	774.50	19060	734.54	24650	835.34	22620	800.21

* Results obtained for the homogenous boundary condition (3) on the outer sides of the domain

** Results obtained for the constant temperature boundary condition $T=T_0(x,y)=283.15$ K on the outer sides of the domain

Moreover, the two last rows of tab. 8 show the results obtained for the homogenous and constant temperature boundary conditions on the left-hand, right-hand and bottom sides of the computational domain in fig. 2(b). When comparing these two rows, it appears evident that these boundary conditions can be used equally for the most common winter conditions.

From an economic point of view, the results and discussion presented above makes clear that the option for early repayment of the proposed innovative solution is possible. If the 110 kV underground cable line is already installed in accordance with fig. 2(b), if the cable trench is completely filled with quartz sand, and if it is planned to coat the pavement surface with, for instance, a cool pavement seal that costs about 3.7 \$/m^2 and lasts up to 7 years [3,21], the appropriate repayment period can be reliably estimated for an electricity transmission tariff of 0.36 \$c/kWh [22]. According to [3,21], two coats of a seal coating could cost an estimated 4440 \$ per kilometer length of the cable line route. Moreover, taking into account the aforementioned transmission tariff and assuming that the power factor equals 0.8, the possible annual total benefit associated with the difference in the transmitted power is 22944.463 kW × 8760 h/y × 0.0036 \$/kWh = 723576.59 \$/y. If the considered underground cable line is 5 km in length, the total cost for the cool pavement seal of 22200 \$ will be paid back in only 268.8 hours of exploitation. Based on this, it is evident that any cost for periodic cleaning, maintenance or resurfacing will be quickly paid back by the proposed innovative solution.

Conclusions

The most important conclusions that can be drawn from the presented results are:

- If the pavement over the cables is coated with white paint or made of a material whose surface absorbs less heat from the sun than it emits to the ambient, then the ampacity of the considered 110 kV cable line can be increased by 6.2 to 25.4 % in summer and by 2.1 to 8 % in winter.
- Cool pavements can be used for controlling the thermal environment of underground cable lines in order to increase their ampacities.
- The proposed innovative solution is new, it does not have to be expensive, it can be easily implemented within current practice, it would result in significant financial benefits and it would be quickly paid back in full.

- The temperatures of the pavement, bedding and cables' conductors decrease with decreasing the ratio of absorptivity to emissivity.
- The thermal effect of the heating pipeline increases with decreasing the ratio of absorptivity to emissivity and decreases with increasing the cable bedding size.
- The effect of the heating pipeline on an underground cable line can best be illustrated using the 50, 60 and 70 °C isotherms and the sizes of the dried, dried-out and extremely-dried-out zones enclosed by the given isotherms.
- The heating-pipe duct behaved as a cooler under the most unfavorable ambient conditions and decreased the cable ampacity by about 36 A for the most common winter conditions.
- The proposed new method for controlling the thermal environment of underground cables is also applicable to the steady-state (or transient) thermal analysis of hot spots where the minimum separation distances (for parallel routing, right angle crossing and approaching) between underground cable lines and heating pipelines (or other power cables laid in cable ducts, cable beddings, pipes etc.) are not fulfilled.

Acknowledgements

This paper was based on research conducted within the project TR33046 funded by the Ministry of Education, Science, and Technological Development of the Republic of Serbia.

Nomenclature

Variables and coefficients

d_1 – conductor diameter, [m]
h – heat transfer coefficient due to convection, [$Wm^{-2}K^{-1}$]
I – load current, [A]
I_{cp} – cable ampacity, [A]
k – thermal conductivity, [$Wm^{-1}K^{-1}$]
n – length of the normal vector $\vec{n}$, [m]
$Q_{S,s}$ – solar irradiance incident on the earth surface, [Wm^{-2}]
Q_v – volume power of heat sources, [Wm^{-3}]
R_{ac} – a.c. resistance per unit length of the conductor, [Ωm^{-1}]
S'_c – geometric cross-section area of the conductor, [m^2]
T – unknown temperature or unknown surface temperature, [K]
T_0 – specified surface temperature, [K]
T_a – air temperature, [K]
T_{cp} – continuously permissible temperature of cables, [K] or [°C]
v_a – wind velocity, [ms^{-1}]
x, y – Cartesian spatial coordinates, [m]
α – solar absorptivity, [–]
ε – emissivity, [–]
σ_{SB} – Stefan-Boltzmann constant, [$Wm^{-2}K^{-4}$]

Abbreviations

AXLJ – single-core power cable with aluminium conductor, extruded cross-linked polyethylene insulation, longitudinally and radial sealed, with polyethylene outer sheath
DIN VDE – Deutsches Institut für Normung Verband Deutscher Elektrotechniker e.V.
FEM – finite element method
HDPE – high-density polyethylene
IEC TR – International Electrotechnical Commission Technical Report
NA2XS(FL)2Y – single-core power cable, N – standardized type, A – aluminium conductor, 2X – cross-linked polyethylene insulation, S – copper screen, FL – longitudinally and crosswise water-tight and 2Y – polyethylene outer sheath
PE – polyethylene
XLPE – cross-linked polyethylene

References

[1] King, S. Y., Halfter, N. A., *Underground Power Cables*, 1st edition, Longman, London and New York, 1982
[2] Mohajerani, A., *et al*., The Urban Heat Island Effect, its Causes, and Mitigation, with Reference to the Thermal Properties of Asphalt Concrete, *Journal of Environmental Management, 197* (2017), July, pp. 522-538
[3] ***, 'Cool Pavement' to Cut Urban Street Heat Gets First California Tryout, *The Urban Climate News, the quarterly newsletter of the IAUC, 64* (2017), June, p. 8
[4] Klimenta, D., *et al.*, Controlling the Thermal Environment of the Underground Power Cables by Means of Public Paved Areas, *Proceedings*, 13th International Scientific – Professional Symposium INFOTEH, Jahorina, Bosnia and Herzegovina, 2014, Vol. 13, pp. 219-224
[5] Al-Saud, M. S., *et al.*, A New Approach to Underground Cable Performance Assessment, *Electric Power Systems Research*, *78* (2008), 5, pp. 907-918
[6] Nahman, J., Tanaskovic, M., Calculation of the Ampacity of High Voltage Cables by Accounting for Radiation and Solar Heating Effects Using FEM, *International Transactions on Electrical Energy Systems*, *23* (2013), 3, pp. 301-314
[7] Salata, F., *et al.*, How Thermal Conductivity of Excavation Materials Affects the Behavior of Underground Power Cables, *Applied Thermal Engineering*, *100* (2016), pp. 528-537
[8] Salata, F., *et al.*, A Model for the Evaluation of Heat Loss From Underground Cables in Non-Uniform Soil to Optimize the System Design, *Thermal Science*, *19* (2015), 2, pp. 461-474
[9] Klimenta, D., *et al.*, Controlling the Thermal Environment in Hot Spots of Buried Power Cables, *European Transactions on Electrical Power*, *17* (2007), 5, pp. 427-449
[10] Klimenta, D., *et al.*, A Thermal FEM-Based Procedure for the Design of Energy-Efficient Underground Cable Lines, *Humanities and Science University Journal - Technics*, *10* (2014), pp. 162-188
[11] International Electrotechnical Commission, IEC TR 62095:2003, Electric cables – Calculations for current ratings – Finite element method, 1st edition, Geneva, Switzerland, 2003
[12] COMSOL, *Heat Transfer Module User's Guide*, Version 4.3, May 2012
[13] International Electrotechnical Commission, IEC 60287-1-1:2006+AMD1:2014 CSV, Electric Cables – Calculation of the Current Rating – Part 1-1: Current Rating Equations (100% Load Factor) and Calculation of Losses – General, 2.1 edition, Geneva, Switzerland, 2014
[14] Çengel, Y. A., *Introduction to Thermodynamics and Heat Transfer*, 2nd edition, The McGraw-Hill Companies Inc., USA, 2008
[15] Andersland, O. B., Ladanyi B., *Frozen Ground Engineering*, 2nd edition, John Wiley & Sons Inc., Hoboken, N.J., USA, 2003
[16] Seemann, S. W., *et al.*, Development of a Global Infrared Land Surface Emissivity Database for Application to Clear Sky Sounding Retrievals from Multispectral Satellite Radiance Measurements, *Journal of Applied Meteorology and Climatology*, *47* (2008), pp. 108-123
[17] Tan, S.-A., Fwa, T.-F., Influence of Pavement Materials on the Thermal Environment of Outdoor Spaces, *Building and Environment*, *27* (1992), 3, pp. 289-295
[18] Smith, J. O., Determination of the Convective Heat Transfer Coefficients from the Surfaces of Buildings within Urban Street Canyons. Ph. D. thesis, University of Bath, Bath, Somerset, UK, 2010
[19] Herb, W. R., *et al.*, All-Weather Ground Surface Temperature Simulation, Project Report No. 478, St. Anthony Falls Laboratory, University of Minnesota, Minneapolis, Minn., USA, September 2006
[20] Gouda, O. E., *et al.*, Effect of the Formation of the Dry Zone around Underground Power Cables on their Ratings, *IEEE Transactions on Power Delivery*, *26* (2011), 2, pp. 972-978
[21] Strömmer-Van Keymeulen, K. E., Cool Pavements for The City of Los Angeles – A Cost-Benefit Analysis, A Study Commissioned by Climate Resolve, Los Angeles, Cal., USA, August 2014
[22] Perovic, B., *et al.*, Optimising the Thermal Environment and the Ampacity of Underground Power Cables Using the Gravitational Search Algorithm, *IET Generation, Transmission & Distridution*, Available online: 13 September 2017, DOI: 10.1049/iet-gtd.2017.0954